Optimal Frequency Support by Residential Multi-Port Power Converters

Iason Kalaitzakis
School of Electrical and Computer Engineering,
Technical University of Crete
Chania, Greece, GR-73100
ikalaitzakis@isc.tuc.gr

Michail Dakanalis
School of Electrical and Computer Engineering,
Technical University of Crete
Chania, Greece, GR-73100
mdakanalis@isc.tuc.gr

Fotios D. Kanellos
School of Electrical and Computer Engineering,
Technical University of Crete
Chania, Greece, GR-73100
kanellos@ece.tuc.gr

***Abstract*—The increasing penetration of Renewable Energy Sources (RES) introduces the increased need for better frequency support to the grid. Decentralized Energy Resources (DER), such as residential prosumers, can sufficiently provide ancillary services to the network. In this paper, the optimal power management of a smart residence during frequency support mode of operation is proposed. The residence comprises an electric vehicle, a battery pack, RES and loads with demand response capabilities. A Multiport Power Converter (MPC) interfaces the aforementioned modules and the power grid. An optimization algorithm is used to calculate the optimal power setpoints of the MPC ports in order to maximize flexibility of the system while satisfying all goals and constraints.**

Keywords— Electric Vehicles, Energy Storage System, Optimal Power Management, Frequency Support, Demand Response

I. Introduction

Conventional power generation using fossil fuels is becoming unappealing due to economic and climate concern reasons. Meanwhile, the trend of electric power grids is towards a decentralized structure, with DER and RES gradually replacing the conventional power plants. However, due to the intermittency and stochastic behavior of RES and the inverter-coupled nature of DER, the grid is facing issues such as decreased inertia, as well as voltage and frequency instability. Fortunately, Energy Storage Systems (ESS) have also undergone massive growth and deployment throughout the grid. An Energy Management System (EMS) equipped with an ESS (e.g., battery pack) is able to provide frequency support to the grid, by releasing or absorbing active power depending on frequency deviations [1]. Additionally, due to the spread of Plug-in Electric Vehicles (PEV), Vehicle-to-grid (V2G) technology [2] can be used in order to utilize the PEV battery's ability to provide significant amounts of active power very fast to the grid [3], [4], [5]. As for the demand side of frequency support, Demand Response (DR) strategies can be utilized to control flexible loads [6]. It is essential for the grid to lessen the burden during peak demand, since it is the time-slot most likely to exhibit frequency instability.

In this paper, an optimal frequency support algorithm is proposed in order to maximize the flexibility of a residential prosumer equipped with a multiport converter, while considering the constraints of the ESS and the local loads. The goal of the algorithm is to provide the necessary active power regulation to assist the grid at the time of considerable frequency deviations, while maintaining to the possible extent the trajectories of the power setpoints of the MPC's ports close the optimal ones obtained by the EMS prior to the disturbance.

As shown in Fig. 1, the PEV, the battery pack, the local loads and a PV array are connected to the MPC, which in turn interfaces them with the power grid. A Phase-Locked Loop (PLL) module is used to measure the grid's frequency, and detect frequency deviations. This information is then fed to a droop module which calculates the overall change of active power (ΔP_{grid}) the EMS needs to apply in order to support the grid's frequency. Afterwards, the frequency support optimization controller calculates the optimal dispatch of the required power change to the four modules. This optimization requires several inputs, such as maximum and minimum power thresholds of each module, maximum capacity and current State of Charge (SoC) of the batteries, load shifting capability etc.

The initial optimal trajectories of the power setpoints of system components are calculated using Particle Swarm Optimization (PSO), presented in earlier work [4]. The EMS uses a time step of 30 minutes, and since frequency instabilities usually last a few minutes, the obtained setpoints are usually constant during the time horizon of the frequency support mode of operation. The calculated optimal trajectories are fed to the real-time control circuits of the four MPC ports as well as the optimal frequency support controller.

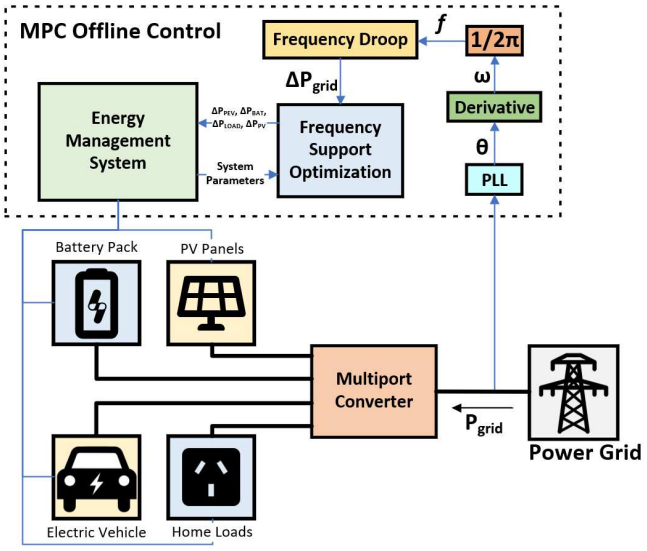

Fig. 1. Block Diagram of the EMS and the MPC's topology

II. Formulation

A. Frequency Droop Control

The first step to provide frequency support to the grid is to detect frequency instabilities and calculate the necessary active power injection or absorption required by the grid. As seen in Fig. 1, the PLL module is fed the grid-side voltage measurement. Using the phase angle θ calculated by the PLL, we can obtain grid frequency. A frequency droop control is applied to calculate the required power change

since it features great performance, adaptability and compatibility with the respective grid code requirements [7], [8].

In the droop characteristic of Fig 2, the frequency dead-band is set between f_2 and f_3, meaning that any fluctuations between those two values do not require frequency support. However, once the frequency deviates between f_3 and f_4 or f_1 and f_2, the droop controller outputs the active power change setpoint, $\Delta P_{grid,}$ according to the frequency deviation amplitude. For any frequency values above f_4 or below f_1, the controller outputs the ceiling or floor of ΔP_{grid} accordingly. The used frequency-power droop curve is defined as it follows:

$$\Delta P_{grid}(f) = \begin{cases} \Delta P_{grid,min} & f < f_1 \\ \Delta P_{grid,min} - \dfrac{\Delta P_{grid,min}}{f_2 - f_1}(f - f_1) & f_1 \le f \le f_2 \\ 0 & f_2 \le f \le f_3 \\ \dfrac{\Delta P_{grid,max}}{f_4 - f_3}(f - f_3) & f_3 \le f \le f_4 \\ \Delta P_{grid,max} & f > f_4 \end{cases} \quad (1)$$

$$\Delta P_{grid,max} = P_{grid,max} - P_{grid}(t'') \quad (2)$$

$$\Delta P_{grid,min} = P_{grid,min} - P_{grid}(t'') \quad (3)$$

Where ΔP_{grid} stands for the deviation from the set-point of the power at the time t'' that frequency support mode of operation is activated. Similarly, $\Delta P_{grid,max}$ and $\Delta P_{grid,min}$ correspond to the maximum and minimum power deviation the residential prosumer can provide. The values of $P_{grid,max}$ and $P_{grid,min}$ are derived from the maximum amount of power the MPC can absorb from/inject into the grid. The dead-band range and the floor and ceiling of the droop characteristic are set as follows:

$f_1 = 49.2$ Hz, $f_2 = 49.8$ Hz, $f_3 = 50.2$ Hz, $f_4 = 50.8$ Hz

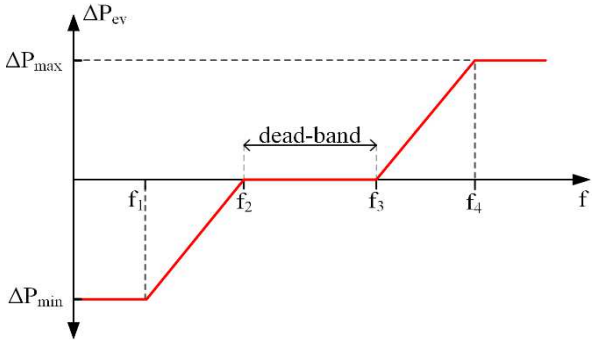

Fig. 2. Droop frequency control characteristic

B. Optimal Frequency Support Algorithm

The optimization algorithm used in this paper to determine the maximum flexibility optimal power dispatch among the four modules of the residential prosumer for uses the built-in MATLAB function fmincon. The fmincon algorithm is a gradient-based optimization method that determines the constrained minimum of linear or nonlinear functions. It is widely used in energy systems due to its high computational speed and reliability [9], [10].The formulation of the constrained optimization problems that can be solved by fmincon is provided in the following.

$$\min f(x) \; such \; that \begin{cases} c(x) \le 0 \\ ceq(x) = 0 \\ A \cdot x \le b \\ Aeq \cdot x \le beq \\ lb \le x \le ub \end{cases} \quad (4)$$

Where A, b, Aeq, beq, ub and lb are matrices and vectors used to formulate the system equality and inequality linear or nonlinear constraints.

In this paper, the objective function is defined as the sum of the weighed flexibilities of the examined system's modules as it follows:

$$\max \sum_i w_i \cdot flex_i(t) = \max \begin{pmatrix} w_{EV} \cdot flex_{EV}(t) + \\ w_{bat} \cdot flex_{bat}(t) + \\ w_{load} \cdot flex_{load}(t) \end{pmatrix} \quad (5)$$

It should be noted that the PV system flexibility is not part of the objective function, as reducing its output is not economically preferable and is left as a last resort, in case the batteries and loads feature zero flexibility in changing their powers (15). The flexibilities of loads are suitably weighed according to system operator preferences.

C. Flexibility Definition

The flexibility of each module in this paper is defined by its ability to alter its output with regard to the resulting movement towards its operational limits. For the two ESSs, the flexibility is therefore linked to the distance between the resulting SoC and its predetermined bounds.

The flexibility of the local loads is proportional to the ability of the load shifting system to add or shed loads, depending on the needs of the grid. For the purpose of the simulation, it is assumed that the system can increase or decrease loads by a specific percentage of the current load power.

The estimation of the flexibility depends on the sign of the change of the power the MPC exchanges with the grid, ΔP_{grid}. As shown in Fig. 1, it is assumed that the power flow of the system is from the grid to the MPC (load convention). Positive $\underline{\Delta} P_{grid}$ therefore links flexibility with the upper limit of SoC, and negative $\underline{\Delta} P_{grid}$ with the lower limit of SoC.

$$flex_{EV}(t) = \begin{cases} \dfrac{SoC_{EV,max} - SoC_{EV}(t)}{SoC_{EV,max} - SoC_{EV,min}}, & \Delta P_{grid} > 0 \\ \dfrac{SoC_{EV}(t) - SoC_{EV,min}}{SoC_{EV,max} - SoC_{EV,min}}, & \Delta P_{grid} < 0 \end{cases} \quad (6)$$

Where SoC_{max} and SoC_{min} are the upper and lower bounds of the EV battery's SoC (in kWh), and $SoC_{EV}(t)$ is the current SoC. Equation (6) can be used to define the flexibility of the battery pack in an equivalent way.

$$flex_{load}(t) = \begin{cases} \dfrac{P_{load,max} - P_{load}(t)}{P_{load,max} - P_{load,min}}, & \Delta P_{grid} > 0 \\ \dfrac{P_{load}(t) - P_{load,min}}{P_{load,max} - P_{load,min}}, & \Delta P_{grid} < 0 \end{cases} \quad (7)$$

$P_{load,max}$ and $P_{load,min}$ (in kW) are the upper and lower bounds of the power of the flexible part of the load. It should be noted that the flexibilities of the EV and the battery pack are tied to energy while load flexibility is tied to power. Since energy is the integral of power, energy related

flexibilities are expected to be less dynamic than those related to power.

D. System Constraints

The proposed frequency support optimization algorithm should satisfy the following constraints.

$$SoC_{EV}(0) + \sum_{0:dt:t} P_{EV}(t) \cdot dt \le SoC_{EV,max} \ \forall t \quad (8)$$

$$SoC_{EV}(0) + \sum_{0:dt:t} P_{EV}(t) \cdot dt \ge SoC_{EV,min} \ \forall t \quad (9)$$

$$P_{EV}(t) \le P_{EV,max} \ \forall t \quad (10)$$

$$P_{EV}(t) \ge P_{EV,min} \ \forall t \quad (11)$$

$$P_{load}(t) \le P_{load,max} \ \forall t \quad (12)$$

$$P_{load}(t) \ge P_{load,min} \ \forall t \quad (13)$$

$$\Delta P_{grid}(t) = \Delta P_{EV}(t) + \Delta P_{bat}(t) + \Delta P_{load}(t) + \Delta P_{PV}(t) \quad \forall t \quad (14)$$

$$\Delta P_{PV} = \begin{cases} \begin{pmatrix} \Delta P_{grid} - \Delta P_{load,max} - \\ \Delta P_{EV,max} - \Delta P_{BAT,max} \end{pmatrix}, & \Delta P_{grid} > \begin{pmatrix} \Delta P_{load,max} + \\ \Delta P_{EV,max} + \\ \Delta P_{BAT,max} \end{pmatrix} \\ 0, & \Delta P_{grid} < \Delta P_{load,max} + \Delta P_{EV,max} + \Delta P_{BAT,max} \end{cases} \quad (15)$$

Constraints (8) and (9) ensure that EV SoC stays within its upper and lower bounds, while (10) and (11) the respective exchanged active power within its bounds. The maximum load power change is set in constraints (12) and (13), (14) ensures power balance while (15) estimates the necessary PV production reduction when the rest prosumer modules are unable to provide the required power change ΔP_{grid}. Constraints similar with (8)-(11) are also applied to the battery pack.

III. Case Study

Two frequency support scenarios were simulated and they are presented below. In the first scenario (Fig. 3a), the frequency drops down to 49.45Hz while in the second (Fig. 4a), frequency rises up to 50.60Hz. The respective set-points of the required power change, ΔP_{grid}, as calculated by the frequency droop controller are shown in Figs 3b and 4b.

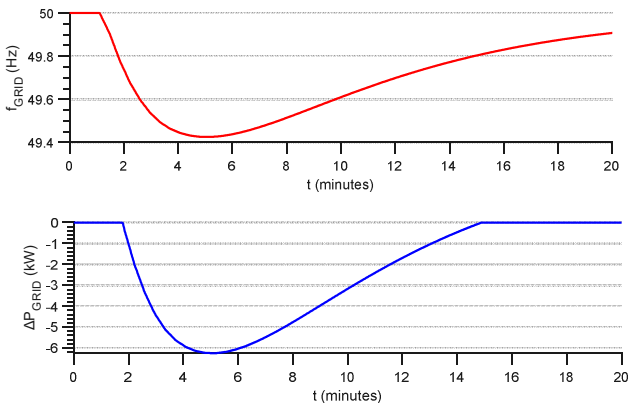

Fig. 3. Frequency and ΔP_{grid} time series during under-frequency

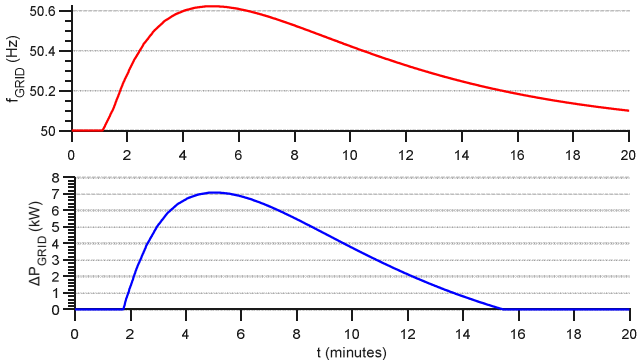

Fig. 4. Frequency and ΔP_{grid} time series during over-frequency

In Table 1, the basic parameters of the used ESSs are listed. The operation limits of the batteries were chosen in a way to maintain SoC between 10% and 90%, to prevent the battery from early aging.

TABLE I. Battery Parameters

	P_{min} (kW)	P_{max} (kW)	SoC_{max} (kWh)	SoC_{min} (kWh)
EV Battery	-5	+5	31.5	3.5
Battery Pack	-5	+5	13.5	1.5

A. Case a): Grid under-frequency

Fig. 5 depicts the power of each prosumer component during under-frequency. As it is shown in Fig. 3, the frequency deviation event occurs at the first minute, while the peak frequency deviation occurs five minutes after the event started.

The objective function weights were chosen in a way to provide less significance to residential load. This is accomplished by setting a smaller value to w_{load} than w_{bat} and w_{EV}. Thus, the first step of the optimization algorithm is to reduce residential load demand. Hence, when residential load response is not enough to ensure ΔP_{grid}, active power is absorbed from the EV battery and battery pack. In the examined case, the EV battery is chosen by the algorithm to contribute more to ΔP_{grid}, as seen in Fig. 5. This is because the initial SoC of EV is higher than the home battery's, and therefore it exhibits higher flexibility. At peak frequency deviation, the EV and residential load cannot ensure the required power change ΔP_{grid}, and the home battery pack supplies the required additional power. Once frequency deviation is over, the components of the residential prosumer return to their normal operation, i.e., follow their power setpoints prior to frequency drop event.

B. Case b): Grid over-frequency

In the examined over-frequency scenario, the initial SoC of the EV battery is almost full, as seen in Fig. 8. Therefore, the EV battery has low flexibility according to (6).

The residential load response obtained in this scenario is shown in Fig. 7. Once flexible load change is unable to ensure ΔP_{grid}, the battery pack and EV battery are dispatched. The EV battery contributes less to ΔP_{grid} during peak frequency deviation, since its SoC is close to the upper limit.

The optimization algorithm was executed on a low-end system, with a runtime of less than half a second for both scenarios.

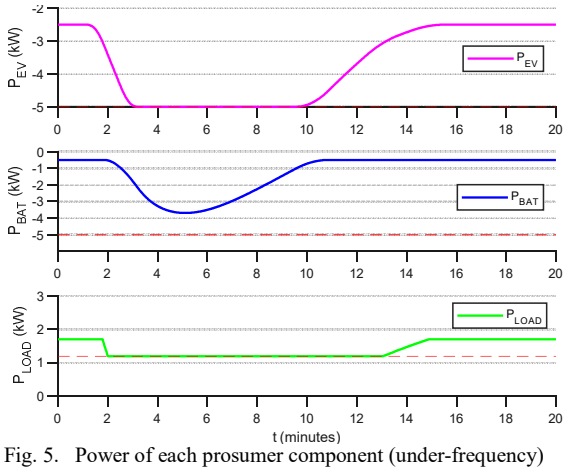

Fig. 5. Power of each prosumer component (under-frequency)

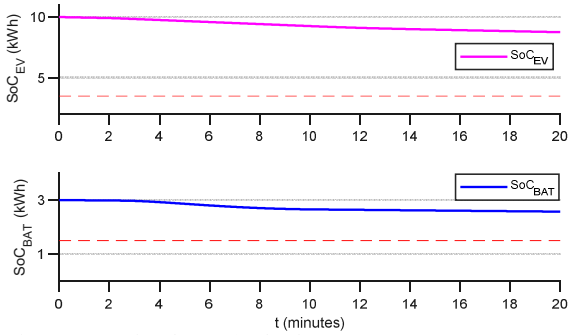

Fig. 6. SoC of each ESS (under-frequency)

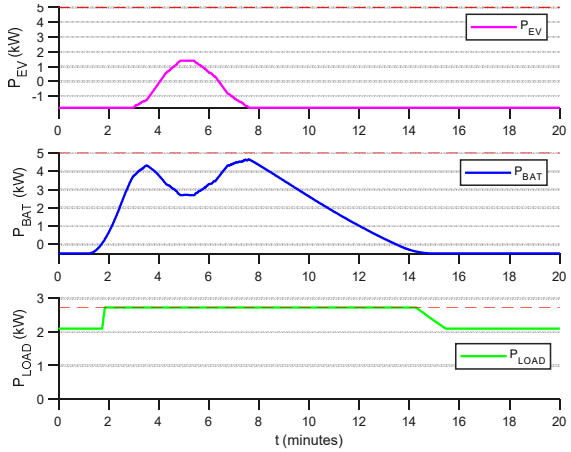

Fig. 7. Power of each prosumer component (over-frequency)

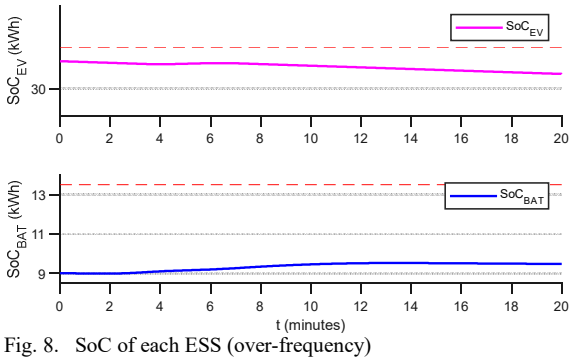

Fig. 8. SoC of each ESS (over-frequency)

IV. Conclusion

In this paper, an optimal frequency support algorithm for a residential MPC with the goal of maximizing system flexibility was proposed. A droop control method was adopted to decide the necessary active power change to support the grid. In order to optimally dispatch the calculated power change to each MPC module the fmincon solver was employed. It was demonstrated that for under-frequency and over-frequency events, the algorithm operates optimally each component of the residential prosumer with respect to their flexibilities and constraints. Additionally, the proposed method was proven to be computationally fast and simple.

Future work may include the addition of ancillary services other than frequency support, as well as the expansion of the examined method to a multi-agent system with multiple smart residential prosumers.

Acknowledgment

This research has been co-financed by the European Regional Development Fund of the European Union and Greek national funds through the Operational Program Competitiveness, Entrepreneurship and Innovation, under the call RESEARCH - CREATE - INNOVATE (project code: T2EDK-01775).

References

[1] E. Barklund, N. Pogaku, M. Prodanovic, C. Hernandez-Aramburo and T. C. Green, "Energy Management in Autonomous Microgrid Using Stability-Constrained Droop Control of Inverters," *IEEE Transactions on Power Electronics,* vol. 23, no. 5, pp. 2346-2352, Sept. 2008.

[2] R. Rana, M. Singh and S. Mishra, "Design of Modified Droop Controller for Frequency Support in Microgrid Using Fleet of Electric Vehicles," *IEEE Transactions on Power Systems,* vol. 32, no. 5, pp. 3627-3636, Sept. 2017.

[3] V. Vai, E. Gladkikh, M. .. -C. Alvarez-Herault, B. Raison and L. Bun, "Study of low-voltage distribution system with integration of PV-battery energy storage for urban area in developing country," *2017 IEEE International Conference on Environment and Electrical Engineering and 2017 IEEE Industrial and Commercial Power Systems Europe (EEEIC / I&CPS Europe),* pp. 1-6, 2017.

[4] L. I. Dulău and D. Bică, "Optimization of a power system with distributed generation sources," *2015 13th International Conference on Engineering of Modern Electric Systems (EMES),* pp. 1-4, 2015.

[5] W. Liu, G. Geng, Q. Jiang, H. Fan and J. Yu, "Model-Free Fast Frequency Control Support With Energy Storage System," *IEEE Transactions on Power Systems,* vol. 35, no. 4, pp. 3078-3086, July 2020.

[6] F. D. Kanellos, "Optimal Scheduling and Real-Time Operation of Distribution Networks With High Penetration of Plug-In Electric Vehicles," *IEEE Systems Journal,* vol. 15, no. 3, pp. 3938-3947, Sept. 2021.

[7] I. Kalaitzakis, M. Dakanalis and F. D. Kanellos, "Optimal Power Management for Residential PEV Chargers with Frequency Support Capability," *2021 10th International Conference on Modern Circuits and Systems Technologies (MOCAST),* pp. 1-4, 2021.

[8] B. Lundstrom, S. Patel, S. Attree and M. V. Salapaka, "Fast Primary Frequency Response using Coordinated DER and Flexible Loads: Framework and Residential-scale Demonstration," *2018 IEEE Power & Energy Society General Meeting (PESGM),* pp. 1-5, 2018.

[9] W. Kempton and J. Tomić, "Vehicle-to-grid power implementation: From stabilizing the grid to supporting large-scale renewable energy," *Journal of Power Sources,* vol. 144, no. 1, pp. 280-294, 2005.

[10] M. Dakanalis and F. D. Kanellos, "Efficient Model for Accurate Assessment of Frequency," *Inventions,* vol. 6, 2021.